

Three-layer Regulation Leads to Monoallelic Olfactory Receptor Expression

Xiao-Jun Tian^{1,†}, Hang Zhang^{2,†}, and Jianhua Xing^{1,*}

¹Department of Computational and Systems Biology, School of Medicine, University of Pittsburgh, Pittsburgh, PA, 15260, USA

²Genetics, Bioinformatics, and Computational Biology Program, Virginia Polytechnic Institute and State University, Blacksburg, VA, 24060, USA

[†]The two contributed equally

*To whom correspondence should be sent: xing1@pitt.edu

Competing interest: None

Abstract Each mammalian olfactory sensory neuron stochastically expresses only one out of thousands of olfactory receptor alleles and the molecular mechanism for this selection remains as one of the biggest puzzles in neurobiology. Through constructing and analyzing a mathematical model based on extensive experimental observations, we identified an evolutionarily optimized three-layer regulation mechanism that robustly generates single-allele expression. Zonal separation reduces the number of competing alleles. Bifunctional LSD1 and cooperative histone modification dynamics minimize multiple allele epigenetic activation and alleles trapped in incomplete epigenetic activation states. Subsequent allele competition for a limited number of enhancers through cooperative binding serves as final safeguard for single allele expression. The identified design principles demonstrate the importance of molecular cooperativity in selecting and maintaining monoallelic olfactory receptor expression.

INTRODUCTION

Olfaction, or the sense of smell, can be essential for the survival and reproduction of an organism. Thus, most species have evolved a highly sensitive olfactory system. A major functional unit of the olfactory system is the main olfactory epithelium where up to millions of olfactory sensory neurons (OSNs) reside. These OSNs sense odor molecules through transmembrane olfactory receptors (ORs), and transmit electric signals to the brain. OR genes are the largest gene superfamily in vertebrates. There are ~60 OR genes in *Drosophila*, 100-200 in fish, ~ 1,300 (including ~20% pseudogenes, *i.e.*, dysfunctional genes that have lost protein-coding ability) in mouse and ~ 900 (including ~63% pseudogenes) in humans (Glusman et al. 2001, Zhang and Firestein 2002, Godfrey, Malnic, and Buck 2004, Vosshall et al. 1999, Nei, Niimura, and Nozawa 2008).

In their classical studies (Buck and Axel 1991, Ressler, Sullivan, and Buck 1993, Chess et al. 1994, Vosshall et al. 1999), Axel, Buck and coworkers showed that in mammals an individual OSN only stochastically expresses one type of functional ORs, or more precisely one allele of the gene. This monoallelic expression of OR proteins with rare violations has also been shown in other organisms such as zebrafish, and is essential for specificity and sensitivity of olfactory sensing. Expression of more than one type of OR would lead to improper stimulation and wiring of the olfactory system and thus misinterpretation of chemical signals (Magklara and Lomvardas 2013).

The above observations raise one of the most intriguing puzzles in neurobiology that remains elusive after several decades of intensive investigations: how is a single allele selected for

activation from a large number of possible OR genes and maintained throughout the lifespan of the neuron? While accumulating evidences and several theoretical studies reveal that a selection is maintained through a feedback loop elicited by expression of the chosen functional OR gene to inhibit further activation of other OR genes (Lewcock and Reed 2004, Serizawa et al. 2003, Nguyen et al. 2007, Dalton, Lyons, and Lomvardas 2013, Lyons et al. 2013, Tan, Zong, and Xie 2013, Alsing and Sneppen 2013, Kolterman, Iossifov, and Koulakov 2012), proposals on the selection mechanism can be divided into two categories: individual-allele centered selection, and enhancer-regulated selection.

The individual-allele centered proposal emphasizes that properties and dynamics within a single allele lead to the single-allele expression. Indeed, the epigenetic signature of an active OR allele in mice converts from H3K9me3, a covalent histone mark typically repressing gene transcription, to H3K4me3, a mark typically activating gene transcription, and this change is likely conserved in mammals (Magklara et al. 2011). Similar epigenetic regulation was reported in zebrafish and *Drosophila* (Sim et al. 2012, Ferreira et al. 2014). Furthermore, disruption of either histone methyltransferases or demethylases leads to violations of the rule of one-allele-activation (Lyons et al. 2013, Lyons et al. 2014, Ferreira et al. 2014). Together with the observation that during OSN differentiation a histone demethylase LSD1 is transiently expressed, an individual-allele centered model suggests a competition among OR alleles for the H3K9me3-to-H3K4me3 transition (see Figure 1A) (Lyons et al. 2013).

In comparison, the enhancer-regulated selection proposal is based on the observations that multiple regulatory genome sequences, *i.e.*, enhancers, can associate with OR promoters (Lomvardas et al. 2006, Khan, Vaes, and Mombaerts 2011, Fuss, Omura, and Mombaerts 2007). Specifically, multiple enhancers bind to the active OR alleles, but not the silenced ones, and form

a dense interaction network, possibly mediated by DNA and histone binding proteins such as transcription factor Bptf (Markenscoff-Papadimitriou et al. 2014). Therefore the enhancer-regulated selection model propose that these enhancers act as *cis* or *trans* elements during the OR selection process.

Each of the two proposed mechanisms has experimental supports and complications. The individual-allele epigenetic competition model reveals a natural feedback mechanism that expression of the winning allele causes endoplasmic reticulum stress and expression of Adcy3 enzyme, which then down-regulates LSD1, leading to an epigenetic trap that stabilizes the OR choice.(Lyons et al. 2013). Theoretical analyses demonstrate the feasibility of this model (an epigenetic race followed by a negative feedback) to generate single-allele expression (Tan, Zong, and Xie 2013, Alsing and Sneppen 2013). The epigenetic competition model, however, also leaves unanswered questions. First, LSD1 functions counter-intuitively as a bifunctional demethylase. Because it removes both the activating methylation mark from H3K4 and the repressive methylation mark from H3K9, it seems not an efficient way to activate ORs. This bifunctional LSD1 is not taken into account in previous model studies. Furthermore, the mechanism may cause accumulation of "semi-converted" OR genes. A typical OR gene including the regulatory region has ~ 40 nucleosomes as inferred from the transgene experiments (Plessy et al. 2012), then the stepwise propagation of conversion in epigenetic marks through an OR gene likely takes longer time than other related processes including gene transcription and translation (Hathaway et al. 2012). Consequently by the time LSD1-induced epigenetic conversion is frozen, one would expect a large number of OR genes in a hybrid state, *i.e.*, with some nucleosomes bearing H3K9me3 and others bearing H3K4me3. Such hybrid state is not normally present in stable cell phenotypes, and extended period of existence in this hybrid state

is likely detrimental for a cell since histone marks can affect higher-order chromatin structures and gene activities (Bannister and Kouzarides 2011). Thus the hybrid state must relax back to the H3K9me3 dominated state. This relaxation, however, places OSNs in a dilemma, since a sufficiently high level of LSD1 is necessary for removing the H3K4 methylation, but would destabilize the epigenetic state of the activated OR gene as well. On the other hand, for an enhancer-based model the molecular mechanism for negative feedback is unclear. Furthermore, all OR genes share similar promoter sequence and regulatory elements, which suggests that specific binding to regulatory DNA sequence alone may not be sufficient to regulate OR selection (Alexander and Lomvardas 2014).

The present work aims to reconcile the above two proposals and provides a mechanistic explanation on single-allele OR expression. Our analysis starts with the hypothesis that OSNs have evolved an optimal strategy for olfactory receptor activation as a multi-task design problem: before differentiation, all OR genes should remain transcriptionally silent; one allele is stochastically selected to become transcriptionally active within a biologically relevant period of time (5-10 days for mice) and the error rate of multiple-allele activation should be minimized; the diversity of activated OR genes should be maximized so each gene has approximately equal probability of being activated; if a pseudo gene is selected, it should be recognized and reselected until a functional allele is chosen; after differentiation the selected allele should be kept transcriptionally active while others remains inactive for the life time of an OSN, which is about 100 days for mice.

Through mathematical and computational analysis, we demonstrate that OSNs achieve the above multi-task problem through synergistic and sequential selection processes governed by the epigenetic competition and enhancer-regulated transcription, respectively. First, multiple alleles

compete for the repressive-to-active epigenetic state transition. Transient expression of the bifunctional LSD1 and cooperativity among nucleosomes lead to an effective two-state transition dynamics, which results in mostly one, occasionally two and rarely more alleles performing such transition, and others remaining predominantly in the repressive epigenetic state throughout the time of competition. Next, while this epigenetic activation is sufficient for OR selection in organisms such as zebrafish, for vertebrates with more sophisticated olfactory sensing, epigenetically active alleles still have to compete for a limited number of enhancers to be transcriptionally active. Cooperative interactions among the enhancers lead to nearly binary OR promoter transcription activity, with negligible probability of having two or more actively expressed alleles simultaneously. Finally the actively transcribed OR induces a negative feedback loop to lower LSD1 level and traps the epigenetic thus transcriptional states of OR alleles.

RESULTS

Mathematical formulation of OR activation

OSNs expressing different subsets of ORs topologically segregate into circumscribed zones. For example, Zone 1 of the mouse main olfactory epithelium contains OSNs that express a subset of 150 OR alleles (Zhang and Firestein 2002). Within each zone, the OR alleles in the corresponding subset are expressed with nearly equal probability (Vassar, Ngai, and Axel 1993, Ressler, Sullivan, and Buck 1993, Shykind et al. 2004). Similar segregated distribution has been found in zebrafish (Weth, Nadler, and Korsching 1996). Zonal segregation reduces the number of OR alleles competing for single allele expression from thousands to hundreds within a zone.

We therefore modeled a cell with 100 alleles to recapitulate the selection process from within a single zone of olfactory epithelium.

First we formulated the following mathematical model for the OR activation problem as illustrated in Figure 1. Throughout this paper for simplicity of presentation we treat the OR genes within a cell as a number of individual alleles. Each OR allele consists of a linear array of $N = 41$ nucleosomes, and each nucleosome can bear repressive H3K9 (R), no (E), or active H3K4 (A) methylations. Transition between these states is governed by enzyme concentration dependent rates. Specifically, demethylation $R \rightarrow E$ and $A \rightarrow E$ can take place either through stochastic exchange between nucleosome histones and the reservoir of unmarked histones with a turnover rate constant d , or through demethylation reactions with rates proportional to concentration of the catalyzing enzyme LSD1. We analyzed the real system that bifunctional LSD1 catalyzes both H3K4 and H3K9 demethylation, and a hypothetical system in which unifunctional LSD1 only catalyzes H3K9 demethylation for comparison. To maintain stable collective epigenetic state of an allele, previous studies reveal that the methylation state change on a nucleosome needs to be influenced by the methylation states of other nucleosomes beyond immediate neighbors (Dodd et al. 2007, Zhang et al. 2014). Therefore we set the methylation rate constants k_1 and k_2 as functions of methylation states of other nucleosomes: k_1 (k_2) is promoted by H3K4 (H3K9) methylation in other nucleosomes, and the influence decreases with the nucleosome spatial separation. Details of the model are given in the Method section.

We propagated the nucleosome methylation states using stochastic Gillespie simulations, and simultaneously updated the levels of the expressed OR protein, Adcy3, and LSD1 by solving deterministic rate equations shown in Figure 1B. We assumed that the gene is only

transcriptionally active when the fraction of nucleosomes bearing active marks, λ , is larger than a threshold value λ_θ .

Low Noise and lack of demethylases kinetically freeze allele epigenetic state before and after differentiation

We first examined the model under conditions prior to and after OSN differentiation. As illustrated by the simulated trajectories in Figure 2A, cooperation among nucleosomes biases them to have the same histone marks. This cooperation leads to collective epigenetic state dominated by either repressive or active marks, which is consistent with previous studies (Zhang et al. 2014, Dodd et al. 2007). Increasing LSD1 concentration (Figure 2A & B) or the level of system noise due to stochastic histone turnover (Figure 2 supplement 1) facilitates removal of existing methylation marks on a nucleosome and thus destabilizes the collective epigenetic states. Therefore, prior to and after differentiation, maintaining high levels of methyltransferases and low level of demethylases forces an allele to be kinetically trapped at one of the two possible epigenetic states throughout the life time of an OSN, analogous to a system trapped (or frozen) in a double-well shaped potential with a very high barrier (see Figure 2C).

Elevation of bifunctional demethylase level leads to a barrier-crossing like dynamics

Next we analyzed OSN differentiation with bifunctional LSD1. As shown in Figure 3A, after elevation of the LSD1 concentration at time 0, the OR alleles remain as repressive mark dominated, until one allele becomes active mark dominated, which leads to the corresponding OR expression and subsequent Adcy3 expression. Adcy3 down regulates LSD1, then the system maintains at a steady state with one OR allele active and the remaining ones inactive. Notice that the inactive alleles remain H3K9me3 dominated throughout the time. Due to stochasticity of the

histone modification process, sampling over 1000 cells gives a broad distribution of T_1 , the time of having the first allele epigenetically active, ranging from a few to 20 or more days and roughly centered around day 8 (Figure 3B). Throughout their lifespan most of the OSNs only have one allele epigenetically activated, while a small fraction has two and rarely 3 alleles epigenetically activated (Figure 3C), consistent with the functional requirements and experimental observations.

Close examination of the simulated trajectories reveals a simple mechanistic explanation illustrated in Figure 3 supplement 1A. Starting with the repressive mark dominated state, transient increase of LSD1 after initiation of OSN differentiation demethylates nucleosomes, and allows resetting of methylation states in the nucleosomes. As a consequence, small patches of H3K4me3 nucleosomes may form, but are flanked by extended regions of H3K9me3 nucleosomes. Such H3K4me3 patches are unlikely to expand because of the cooperativity of methylation between nucleosomes and the dominance of H3K9me3 marks at the current stage. Nevertheless, when an H3K4me3 patch reaches a critical size -- as a rare event, it is able to propagate spontaneously and generate an epigenetic conversion of the OR gene into the H3K4me3 dominated state. That is, LSD1 increase resembles lowering the transition barrier between the double-well shaped potential shown in the previous section, and allows rare transition to happen (Figure 3D). Once one allele converts to the H3K4me3 dominated state, and triggers the negative feedback loop to remove LSD1, the system is kinetically trapped again with high transition barrier. The converted allele is kept active with H3K4me3 marks, while the remaining alleles bear repressive H3K9me3 marks. A prominent feature of this barrier-crossing-like dynamics is that throughout the process the probability of having an allele with hybrid pattern of epigenetic marks is low, and most alleles only fluctuate around the H3K9me3

dominated state.

Based on the above analogy to a double-well potential, we reasoned that increasing the LSD1 concentration facilitates epigenetic state transitions. Indeed simulation results show that upon increasing the LSD1 concentration, $\langle T_I \rangle$, the average of T_I , decreases (Figure 3E), but the fraction of cells with multi-allele activation increases (Figure 3F). Lyons et al. also observed fewer mature OSNs in mice with reduced LSD1 (Lyons et al. 2013), as what predicted in Figure 3E. Therefore a given organism may have evolved an optimal LSD1 concentration to compromise the requirements of single-allele activation and efficient OSN differentiation.

Next we asked how the number of permitted alleles affects the ratio of single allele activation (Figure 3 supplement 1B). The ratio first increases since a cell with more alleles has higher probability to have at least one allele epigenetically activated during the differentiation period. Then it decreases after a peak value since the probability of having more than one allele activated also increases with the number of alleles per cell. While the exact position of the peak depends on model parameters, the model results predict that the number of OR genes within a zone is under selective pressure.

Elevation of unfunctional demethylase level leads to ratchet-like dynamics

The dynamics is completely different if a hypothetical LSD1 only removes repressive marks during differentiation. As revealed by a typical simulated trajectory (Figure 4A), starting at time 0 all the OR alleles begin to remove repressive marks and gain active marks, while some are faster than the others. After one epigenetically active OR allele activates the feedback loop and lowers the LSD1 concentration, some OR alleles return to the epigenetically repressive state, and a number of others propagate further to the epigenetically active state. A significant fraction of

alleles are present in some hybrid epigenetic state during the activation process, and subsequently retard in the hybrid state due to slow demethylation (Figure 4A & B). In contrast, when LSD1 bifunctions, the probability of catching an allele in an intermediate state is very low (Figure 4B) by the time LSD1 depletes, leading to efficient relaxation. Therefore, bifunctional LSD1 avoids hybrid state by maintaining one single large barrier between the repressive mark dominated and active mark dominated states. While making this comparison, we have chosen model parameters so the distribution of T_l with a unifunctional LSD1 also centers roughly around day 8 (Figure 4C). Then sampling over 1000 cells shows that ~ 87% of the cells have two or more alleles activated at the end of differentiation (Figure 4D). These simulation results demonstrate that the hypothetical unifunctional LSD1 scheme is not as robust as the bifunctional enzyme scheme on achieving single allele epigenetic activation.

Again the above dynamics of allele selection has a simple mechanistic explanation (Figure 4 supplement 1A). Let us start with an allele originally in the H3K9me3 dominated state. Increased LSD1 level promotes empty nucleosomes. Following the same argument in the previous section, an empty nucleosome still has higher probability to add H3K9me3 compared to H3K4me3. However, once an H3K4me3 is added, the removal rate is very low. Consequently, the dynamics is ratcheted (Peskin, Odell, and Oster 1993) towards increasing the number of nucleosomes with H3K4me3, as illustrated by Figure 4E. A prominent feature of this ratchet-like dynamics is that every allele has its total number of H3K4me3 nucleosomes increasing with time, with a leading allele followed by other alleles on the way of converting their nucleosome marks, thus intuitively it is difficult to ensure single allele epigenetic activation.

Mathematically controlled comparison explains why bifunctional LSD1 improves the ratio of single allele activation.

To understand why the effective two-state barrier-crossing dynamics is advantageous over the multi-state ratchet-like dynamics on generating single allele activation, we performed further mathematical analysis based on the following reasoning. In the OR system a number of alleles convert their epigenetic state independently and stochastically under an elevated LSD1 concentration. Let us denote the activation time separation between the first two converted alleles as τ . Then from an engineering perspective, a better design to achieve single-allele activation is the one with a larger τ , which means that the two activation events are better separated temporally, and thus more time for the first allele to elicit the feedback loop and prevent activation of another allele.

Therefore we performed mathematically controlled comparison among a set of simple models shown in Figure 4 supplement 1B. Consider two alleles transiting independently from the repressive mark dominated state to the active mark dominated state through various numbers of intermediate states, but with the same mean first arrival time. Figure 4 supplement 1C shows that the two-state model has an exponentially shaped first-arrival-time distribution f_2 , while those with $(n - 2)$ intermediate states have peaked ones that at large t decrease faster with increasing n . One can randomly draw two points p_{t1} and p_{t2} from a distribution, corresponding to the stochastic activation events of the two independent alleles. Clearly the temporal separation of the two points, τ , is likely to be larger if they are drawn from a broader f corresponding to smaller n . Indeed Figure 4 supplement 1D shows that the distribution of τ has longer tail for smaller n . That is, a design with the two-state dynamics is better than that with the multi-state dynamics.

Epigenetic competition model predicts zebrafish but not mouse experiments on inhibiting methyltransferases/demethylases

In the illustrative double-well potential shown in Figure 3D, lifting the left well allows easier transition to the right well thus higher probability of multiple allele activation, while elevating the barrier height leads to an opposite effect. Experimentally, shallowing of the left well can be realized by reducing the enzymatic activity of H3K9 methyltransferases, G9a and GLP. Similarly decreasing LSD1 concentration corresponds to increasing the barrier height. The simulation results in Figure 5A show that reducing the LSD1 concentration ($LSD1^R$) impedes OR activation, which can be partially restored by decreasing the enzymatic activities of H3K9 methyltransferases ($LSD1^R/E_{K9M}^R$), consistent with that observed in mice (Lyons et al. 2014). Furthermore, partially inhibiting the enzymatic activities of G9a/GLP (E_{K9M}^R) leads to increased number of cells coexpressing multiple ORs, which is confirmed in zebrafish (Ferreira et al. 2014).

When the left well in Figure 3D lifts further the system resembles more and more that in Figure 4E, and the epigenetic activation process evolves from a barrier-crossing-like dynamics to a ratchet-like dynamics. The simulated results in Figure 5 supplement 1A & B indeed predict that in contrast to that in wild type (WT), with further reduced level of H3K9 methyltransferases (E_{K9M}^{RR}) a majority of the OR alleles assume a hybrid methylation pattern during the differentiation process, and thus significant increase of multi-OR activation (Figure 5A). However, experimental studies using G9a/GLP double knockout (dKO) mice only observed elevated but still rare multi-OR coexpression compared to the WT control in mice (Lyons et al. 2014). Therefore the epigenetic conversion mechanism is insufficient to explain the experimental results.

Competition of cooperatively bound enhancers further reduces coexpression of multi-allele ORs.

To explain the G9a/GLP dKO mouse experiment, we generalized the model based on recent studies (Markenscoff-Papadimitriou et al. 2014, Lyons et al. 2014). We hypothesize that for terrestrial vertebrates such as humans and mice, active expression of an OR allele requires both the gene bearing active epigenetic marks (H3K4me3) and co-localization of a sufficient number of enhancers to the allele. In the following, we elaborate on how we model this process.

Suppose M enhancers are available for an OR genomic cluster with L OR alleles (see Figure 5B). Each enhancer can bind to the epigenetically active l -th OR allele with a free energy of binding ε_l , and can interact with any other enhancer bound to the same allele with energy ζ . Enhancer binding to alleles with repressive marks is weak and can be neglected (Markenscoff-Papadimitriou et al. 2014). Notice that enhancer binding to active alleles is cooperative: when two or more epigenetically active alleles compete for the enhancers, an enhancer prefers to binding to the one that already has more enhancers bound since it can form more enhancer-enhancer interactions. Consequently, enhancers collectively bind to and transcriptionally activate one allele at a given time, and switching from binding to one allele to another one is rare since it requires breaking many interactions. While the exact value of M is currently not known, the experimental observation that ectopically introduced multiple copies of a specific H enhancer increase the probability of multi-OR coexpression (Lomvardas et al., 2006) supports our assumption: alleles have to compete for an unsaturating number of enhancers in WT cells; due to cooperative binding the enhancers first saturate one allele and then extra enhancers bind to others.

We then performed Gillespie simulations for the enhancer-allele binding/unbinding dynamics. Figure 5C&D give an example of a cell with two alleles becoming epigenetically active (Figure 5C), but only one of them is transcriptionally active at a given time (Figure 5D). If the enhancers bind to the two alleles with equal strength, *i.e.*, ζ and ε_l assume the same values for different

alleles and enhancers, the enhancers jump stochastically and collectively between the two alleles, showing a two-state dynamics alike a particle moving in a symmetric double-well potential (left panel of Figure 5D). The frequency of transitions depends on the actual binding strength and the number of enhancers. However, it is likely that the values of ζ and ε_l are slightly allele-dependent. Then cooperative enhancer binding can amplify this difference by many folds. For example, suppose that there exists a free energy difference of enhancer-allele binding $\Delta\varepsilon = \varepsilon_1 - \varepsilon_2$ between allele 1 and allele 2. Then the free energy difference between allele 1 bound with M enhancers and allele 2 bound with M enhancers is $M\Delta\varepsilon$, which can be significant due to the factor M . So the allele with stronger enhancer binding dominates transcriptionally alike a particle moving in an asymmetric double-well potential (middle and right panels of Figure 5D).

The above model reaches a surprising prediction on the OR expression pattern when the level of H3K9 methyltransferases is reduced. Compared to WT cells, the cells with E_{K9M}^R tend to have more OR alleles being epigenetic active (Figure 5E), as expected. However, except for a small group of OR genes becoming transcriptionally upregulated, most of them instead show decreased expression compared to those in the WT (Figure 5F). Further reduction of the enzyme level (E_{K9M}^{RR}) causes fewer OR alleles to be expressed, but each with higher expression level (Figure 5F & G). Seemingly counterintuitive, this prediction is what observed experimentally (Lyons et al. 2014).

The reduced diversity in Figure 5F has a simple mechanistic explanation. For illustration purpose let us consider a toy system in which L ($= 4$) OR alleles exist in a zone, and these alleles have strong (allele 1), medium (allele 2), and weak (alleles 3 and 4) binding strength to the enhancers, respectively (Figure 5H). Existing experimental evidences suggest that the epigenetic activation step is stochastic and each allele has roughly equal probability $1/L$ to be chosen. For WT OSNs,

most cells have only one epigenetically active allele, and the allele becomes transcriptionally active as well. Therefore the overall transcriptional probability of each allele in the zone is $\sim 1/4$. On the other hand, with the H3K9 methyltransferase level reduced (E_{K9M}^R and E_{K9M}^{RR} , or G9a KO and G9a/GLP dKO experimentally), an OSN may have multiple epigenetically active OR alleles. For simplicity of argument let us assume that in a cell three alleles compete for enhancers. Since each allele has the same probability becoming epigenetically active, there are 4 possible combinations with equal probability, (123), (124), (134) and (234). As an allele with stronger enhancer binding dominates transcription, one expects that the first 3 combinations mainly express allele 1, and the last one expresses allele 2. That is, the expression of allele 1 is upregulated while that of alleles 3/4 are down regulated. Similarly, with more epigenetically active alleles coexisting in individual OSNs, more OSNs are likely to have the strongest alleles active and express them; fewer OSNs have the chance to express the weaker alleles. Consequently, the OR diversity in the OSN population becomes further reduced.

In the above simulations we assumed that only the number of enhancers bound to an allele affects its transcription. It is possible that enhancers have certain OR gene specificity (Fuss, Omura, and Mombaerts 2007, Lomvardas et al. 2006, Serizawa et al. 2003). Therefore we considered the alternative possibility that only one of the binding enhancers, say enhancer 1, is necessary for activating a given OR gene. Compared to the case with only enhancer 1 (Figure 5 supplement 1C upper panel), with other enhancers being present enhancer 1 shows increased dwelling time of binding to allele 1 and this binding correlates with the overall collective binding state of enhancers (Figure 5 supplement 1C lower panel). That is, the presence of other enhancers stabilizes the binding of the enhancer who actually affects the allele transcription, and the above results discussed in this section still hold in this case.

Model studies identify multiple schemes of OR transcription switching

The trajectories in Figure 5D reveal that an OSN cell occasionally switches off an active OR allele and chooses another one. This switching phenomenon has been widely reported in the literature (Shykind et al. 2004), thus we examined these trajectories in detail.

For WT OSNs, most switching takes place as a pseudo gene allele gets epigenetically and transcriptionally activated first, then a functional allele transcriptionally switches on after certain time (Figure 6A). This is because the products of a pseudo gene fail to elicit the *Adcy3* mediated feedback loop to reduce the *LSD1* level, and permit another allele to be epigenetically activated. Figure 6B shows another type of switch also found in simulations with WT OSNs. A functional allele is activated first and then switches to a pseudogene, the cell reenters to the selection process until an alternative functional is activated. In both two schemes an allele remains epigenetically active even after switching off transcriptionally.

In *Adcy3* KO mice the feedback loop is disrupted and the simulation results in Figure 6C reveal a new switching pattern. First a transcriptional switch takes place between two alleles. Then the newly activated allele switches off epigenetically and thus transcriptional, and the original allele switches back to be transcriptionally active. Mechanistically the sustained high level of *LSD1* in *Adcy3* KO cells leads to collective removal of H3K4 methylation from the activated allele.

Not surprisingly, the switching frequency increases in *Adcy3* KO OSNs compared to that in WT OSNs (Figure 6D) since more cells have multiple epigenetically active alleles. Furthermore, the fraction of cells expressing pseudo ORs increases while that expressing functional ORs decreases in *Adcy3* KO simulations (Figure 6E), consistent with the experimental results (Lyons et al. 2013). Mechanistically in *Adcy3* KO system transcription of a functional allele does not inhibit

further epigenetic activation of pseudo gene alleles, and the latter then competes with the former for transcription.

Therefore the simulations suggest two possible mechanisms for OR allele transcriptional switching. One is that an allele converts from the active H3K4me3 epigenetic state back to the repressive H3K9me3 state. Experimental testing of this mechanism requires monitoring the histone modification state of one allele over time. Another is that the enhancers cooperatively change their binding from one allele to another one, with both being epigenetically active. The present model predicts that the genes showing upregulated expression in the G9a/GLP dKO mice, such as *Olf231*, have slighter stronger interactions with the enhancers than the remaining genes do. Then an experimentally testable prediction is that in normal mice, OSNs that express one of these genes should have lower frequency of switching than those cells express other genes in the same zone do.

DISCUSSIONS

Single allele activation in olfactory sensory neurons is a multi-decade-long puzzle in neurobiology. Recently several mathematical models have been formulated to examine various proposed mechanisms for explaining the phenomenon (Alsing and Sneppen 2013, Tan, Zong, and Xie 2013, Kolterman, Iossifov, and Koulakov 2012). Compared to these existing modeling studies, the present model is based on some key experimental observations available only recently. The model, while coarse-grained, has every of its components corresponding directly to an experimentally measurable quantity, which makes comparison to experimental results and prediction test transparent. More importantly, there are some essential differences between the present model and the existing ones both mechanistically and conceptually.

A sequential three-layer regulation mechanism controls single allele activation.

Through integrating a large body of existing experimental studies, our theoretical studies suggest that single allele activation is achieved through a series of selection processes functioning synergistically (Figure 7). A subset of the alleles is selected by the zonal segregation. Then they are randomly chosen to be epigenetically activated through transient elevation of bifunctional LSD1. Most of the cells only have one epigenetically active and thus transcriptionally active allele. If more than one allele are epigenetically activated, they compete for the enhancers to be transcriptionally active, resulting in only one epigenetically and transcriptionally active allele. If the activated allele is not a pseudo gene, it triggers the feedback to prevent further epigenetic state change. Therefore, this coordinated three-layer regulation mechanism faithfully assures that only one OR allele is expressed in one OSN. All other existing models consider only epigenetic switching or competition for certain regulatory elements. For example, the epigenetic switching model of Alsing et al. (Alsing and Sneppen 2013) states that “singular gene selection does not require transient mechanisms, enhancer elements or transcription factors to separate choice from maintenance”.

The OR selection process is optimized to satisfy hierarchical multi-task and even opposing requirements.

All existing models recognize that OSNs need to achieve monoallelic OR expression. Based on extensive experimental results, the present model further argues that the regulation system is optimized to achieve multi-task functional requirements. Some of these requirements, such as maximum OR diversity and minimal hybrid state, while not recognized in earlier studies,

naturally reconcile many seemingly counter-intuitive and contradictory observations and ideas in the field.

It might seem redundant to have both epigenetic activation and enhancer competition to achieve monoallelic expression. Epigenetic activation selects OR alleles with approximately equal probability, but leads to a small percentage of cells having multiple epigenetically active alleles. On the other hand, enhancer competition is more effective on ensuring single allele activation, but it also introduces strong bias towards allele selection. Therefore, to achieve single allele activation as the top priority and maximize the diversity of expressed ORs at the same time, the OR selection system has evolved a combined procedure. The epigenetic activation step is optimized with a bifunctional LSD1 to achieve maximal single allele activation. When multiple allele epigenetic activation does happen but with low probability, the enhancer competition in allele selection serves as the last “safeguard” without severely distorting the overall diversity of OR expression. Similarly our analysis reveals that other variables are also subject to the multi-task optimization. For example, the LSD1 concentration may be optimized as a result of compromise between maximum single-allele activation and fast allele activation.

Counter-intuitive bifunctionality of the LSD1 maximizes single allele epigenetic activation.

An intriguing feature of the OR selection system is that the selection is initialized then maintained through regulating the level of the bifunctional LSD1. While not discussed in previous studies, our analysis reveals that it is important to remove both repressive and active marks during the activation process. This bifunctionality leads to a barrier-crossing-like dynamics with high single allele epigenetic activation ratio and minimization of alleles trapped in hybrid epigenetic states. Theoretically, one might conceive many possible designs of

modulating the methyltransferases to activate OR in the cell. For example, LSD1 might first remove H3K9 methylation to activate the alleles, subsequently remove H3K4 methylation on those “unsuccessful” alleles including pseudogenes. However, besides problems of the ratchet-like dynamics discussed above, it is also practically difficult to prevent the enzyme from destabilizing the activated allele by removing its H3K4 methylation marks as well.

Therefore a central prediction of our model is that throughout the selection process a “tug-of-war” exists for adding and removing H3K9 and H3K4 methylations. This “tug-of-war” is analogous to that of ultrasensitive phosphorylation-dephosphorylation cycle observed in signal transduction networks (Goldbeter and Koshland 1981), and work together with nucleosome crosstalks to generate the kinetic cooperativity during the epigenetic activation process. Furthermore the enzymatic activities of methyltransferases are in excess over that of demethylase, i.e., LSD1. Lyons *et al.* indeed observed that G9a/GLP at excessive concentration coexist with LSD1 during OSN differentiation (Lyons et al. 2014).

Seemingly subtle differences on the regulation schemes lead to qualitatively different mechanisms.

Existence of a feedback loop has long been recognized to be necessary for maintaining the choice of OR selection. Not surprisingly all mathematical studies including ours contain a feedback loop. These models, however, differ on how the feedback loop is implemented. Figure 7 Supplement 1A-D summarizes the basic structures of the four existing mathematical models. Some of these models differ only in some subtle details, but suggest qualitatively different mechanisms. We have already discussed models with bifunctional and unifunctional LSD1. The two models differ only on whether H3K4 methylation is regulated by the negative feedback loop,

but lead to barrier-crossing versus ratchet-like dynamics. Similarly, the model of Alsing et al. (Alsing and Sneppen 2013) emphasizes that “the only requirement is that the coupling feedback must favour the silent nucleosome state”. Figure 7 Supplement 1E gives a corresponding potential analogy, where activation of the feedback loop stabilizes the repressive mark dominated well, while slightly destabilizes the active mark dominated well. On the contrary, the feedback in the present model modulates the “barrier” without necessarily favoring any of the nucleosome states (Fig. 3D). The two models respond differently to enzyme concentration fluctuations. In that of Alsing et al., fluctuations of any of the methyltransferases or demethylases affect the relative stability of the two states, and these fluctuations are coupled. On the other hand, in the present model fluctuations of the two methyltransferases are largely decoupled provided that the LSD1 concentration is kept low compared to that of the methyltransferases.

The model makes multiple testable predictions and many have been confirmed.

A prominent feature of the present modeling study is that it is not only based on extensive experimental information, but also makes a number of predictions and experimental suggestions. As summarized in Table S1 and discussed above, our model predicts many seemingly “strange” dynamic features of the OR selection system, which have been experimentally observed but remained unexplained. Here we discuss a few of suggested new experiments in detail.

To reach the diversity change prediction in Figure 5F & G, a key ingredient in the model is that the values of ζ and/or ε_l are allele-dependent. The difference may come from DNA sequence, and it may be even less than the thermal energy $k_B T$, the product of Boltzmann’s constant and temperature. However, this free energy difference can be significantly amplified by enhancer

cooperative binding (Figure 5D). This amplification explains why strong OR expression bias occurs in *G9a/GLP* dKO mice while Lyon *et al.* could not identify any significant differences between the promoters of the most upregulated ORs and the remaining ones in predicting the transcription-factor-binding-motifs (Lyons *et al.* 2014). Another possible source of different OR-enhancer binding strength lies in the different distances between enhancers and alleles. Different allele-enhancer distances may require slight different DNA distortion to form the OR-enhancer binding complex, as implied by the observation that moving the H enhancer closer to MOR28 dramatically up-regulates its expression while down regulates other neighboring ORs (Serizawa *et al.* 2003). To further test this mechanism, one can replace an upregulated OR gene and its promoter by a down-regulated one, and test whether the latter becomes upregulated in a *G9a/GLP* dKO main olfactory epithelium. Another suggested experiment is to introduce enhancers ectopically to *G9a* KO mice (Lomvardas *et al.*, 2006), which should at least partially rescue the reduction of OR diversity if the model holds.

To test the prediction given in Figure 5 supplement 1A&B, one may sort GFP⁺ cells from OMP-IRES-GFP control mice and *G9a/GLP* dKO OMP-IRES-GFP mice (Magklara *et al.* 2011), respectively, then perform CHIP-qPCR for selected silent OR genes. We expect that H3K9me3 dominates on silent OR alleles from the control mice, but H3K4 and H3K9 methylations mixed at various extent on silent OR alleles from the dKO mice (Figure 5 supplement 1B). One can further measure the epigenetic pattern at different time points before and after differentiation to test the prediction that it takes long time for the alleles with mixed methylations to relax to a steady state distribution.

Future studies may reveal fine tuned regulation on OR and other allele-specific activation processes.

This work aims at revealing the essential elements that regulate the OR selection process. Therefore we adopted a coarse-grained model without specifying many details. For example, the model requires kinetic cooperativity of epigenetic mark change among nucleosomes, and energetic cooperative binding of a limited number of enhancers. Molecular details of these cooperativities require clarification. For simplicity, we did not distinguish possible differences among enhancers and their OR specificity, and leave the effective enhancer number in a cell as an unspecific parameter. The molecular mechanism for zonal segregation is unclear. All these unresolved questions require further studies.

Besides the mechanisms discussed in this work, living organisms have likely evolved additional mechanisms for fine-tuning OR expression. For example, chromatin structures in OSNs are highly dynamic to expose or sequester specific OR genes. Specific patterns of DNA methylation and other histone covalent modifications have been observed for OR promoters and enhancers. OR genes are not expressed with exact equal probability, and coordinated expression might exist (Rodriguez-Gil et al. 2010). Further studies are needed to reveal these subtle regulation mechanisms.

Our model studies reveal some design principles to achieve robust single allele activation, which may apply to other single allele systems as well (Magklara and Lomvardas 2013). Stochastic monoallelic expression has been widely observed in diploid organisms, with an estimate of >20% of the autosomal genes, and OR expression is one prominent example (Burgess 2014). Further studies can examine whether the regulatory mechanisms discussed here are adopted in other cell types.

METHOD:

Each OSN is modeled to have $N_p = 30$ pseudo gene alleles and $N_f = 70$ functional OR alleles, with the only difference being that the product of the former does not elicit Adcy3 mediated feedback.

Epigenetic dynamics: For simplicity we treated step-wise methylations/demethylations on a nucleosome as single steps, and treated participating enzymes other than LSD1 implicitly. Denote methylation state of a nucleosome R, E, and A as $s = -1, 0, 1$, respectively. We set the methylation rate constants for an empty nucleosome i as

$$k_1^i = k_1^0 \exp\left(\sum_{j \neq i} \frac{\mu}{|i-j|} \delta_{s_j, -1}\right), \quad k_2^i = k_2^0 \exp\left(\sum_{j \neq i} \frac{\mu}{|i-j|} \delta_{s_j, 1}\right),$$

where the sum is over all other nucleosomes, and δ is a Kroneck-delta function. That is, each of the other nucleosomes influences the nucleosome to add the same mark of the latter, and the influence decreases with the nucleosome spatial separation. An insulating boundary is assumed, and three nucleosomes in the middle form a nucleation region with higher enzymatic rate constants than other nucleosomes have. We modeled E_{K9M}^R and E_{K9M}^{RR} by reducing the value of k_2^0 for the WT to 90% and 80%, respectively. A theoretical justification of the model from a more detailed physical model (Zhang et al. 2014) is given below, and values of the model parameters can be found in Table S2.

Three nucleosomes located at the center of the nucleosome array form the nucleation region. Existence of this nucleation region reflects the observation that some DNA sequence specific molecular species, such as transcription factors and noncoding RNAs, help on recruiting histone modification enzymes. We also performed simulations with the nucleation region and the found no qualitative change of the mechanisms discussed in the present paper.

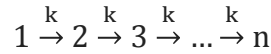
Enhancer binding dynamics: For simplicity we assumed that there is no free enhancer. This assumption is not essential for the present discussions and can be easily removed at the expense of a few additional parameters. Also we treated the enhancers equally, although generalization is straightforward when additional experimental information becomes available. An enhancer can jump from allele i to j with rate, $k_{i \rightarrow j} = v \exp[0.5(\varepsilon_i - \varepsilon_j + (M_i - 1 - M_j)\zeta)]$ to satisfy the detailed balance requirement, where M_i and M_j are the number of enhancers bound to allele i and j before the jump, respectively, and $\sum_i M_i = M$. We chose the factor 0.5 to satisfy the detailed balance requirement, *i.e.*, $k_{i \rightarrow j}/k_{j \rightarrow i}$ equals to the Boltzmann factor corresponding to the system free energy after the transition divided by that prior to the transition. At each Gillespie simulation step, one of all possible enhancer binding changes is randomly selected. Since an allele with higher enhancer binding affinity dominates enhancer competition, for computational efficiency we only simulated enhancer dynamics explicitly for the results in Figure 5D and Figure 5 supplement 1. For other simulations in Figure 5 and 6 we adopted a simplified procedure as schematically illustrated in Figure 5H. That is, we obtained the probabilities of having a cell with various numbers of epigenetically active alleles (Figure 5E), and stochastically ranked the enhancer binding affinities of the 100 alleles, Assuming that each allele has the same probability of being epigenetically active, we consider all the possible combinations and the associated weights of having two or more alleles being epigenetically active, and for each case the allele with strongest enhancer binding affinity is chosen to be transcriptionally active.

Gene expression dynamics: All gene expression is modeled by solving ordinary differential equations (Figure 1B). For simulations with enhancer binding dynamics in Figure 5, 6, we multiplied to the first synthesis term of OR expression a Kroneck-delta function, which assumes 1 if the allele is epigenetically active and other alleles are epigenetically silent, or if its enhancer

binding affinity is stronger than that of other epigenetically active alleles, and 0 otherwise. For Adcy3 KO simulations, k_A is set to be 0. All concentrations are in reduced unit.

Mathematical analysis of simple models

Here we show how to calculate the results in Figure 4 supplement. Consider the process (also shown in Figure 4 supplement B)



Denote p_i the probability of an allele in state I , which is given by

$$\frac{d}{dt} \begin{pmatrix} p_1 \\ p_2 \\ \dots \\ p_n \end{pmatrix} = \begin{pmatrix} -k & 0 & 0 & 0 & 0 \\ k & -k & 0 & 0 & 0 \\ \cdot & \cdot & \cdot & \cdot & \cdot \\ 0 & 0 & 0 & k & 0 \end{pmatrix} \begin{pmatrix} p_1 \\ p_2 \\ \dots \\ p_n \end{pmatrix} \text{ with } \begin{pmatrix} p_1 \\ p_2 \\ \dots \\ p_n \end{pmatrix}_0 = \begin{pmatrix} 1 \\ 0 \\ \dots \\ 0 \end{pmatrix}$$

The solution of the system is,

$$\begin{aligned} p_1(t) &= e^{-kt}, \\ p_2(t) &= e^{-kt} kt, \\ p_3[t] &\rightarrow \frac{1}{2} e^{-kt} k^2 t^2, \\ &\dots \\ p_n[t] &\rightarrow \frac{1}{(n-1)!} e^{-kt} k^{n-1} t^{n-1} \end{aligned}$$

The first-arrival time distribution is $f_n(t) = \frac{d}{dt} p_n(t)$, and f_n is normalized ($\int_0^\infty f_n * dt = 1$).

Then

$$\begin{aligned} f_2[t] &\rightarrow e^{-kt} k^1, \\ f_3[t] &\rightarrow e^{-kt} k^2 t, \\ &\dots \end{aligned}$$

$$f_n[t] \rightarrow \frac{1}{(n-2)!} e^{-kt} k^{n-1} t^{n-2}$$

The mean first arrival time T is given by $T = \int_0^{\infty} f_n * t * dt$. Require that the mean first arrival time T is the same for different n, one has $k = (n-1)/T$.

The formula below gives the distribution that the arrival time difference between two alleles is τ

$$F_n = 2 \int_0^{\infty} f_n(t) * f_n(t + \tau) * dt$$

Thus,

$$\begin{aligned} F_n &= 2 \int_0^{\infty} \frac{1}{(n-2)!} e^{-kt} k^{n-1} t^{n-2} * \frac{1}{(n-2)!} e^{-k(t+\tau)} k^{n-1} (t+\tau)^{n-2} * dt \\ &= 2 \frac{1}{(n-2)! (n-2)!} e^{-k\tau} k^{2n-2} \int_0^{\infty} e^{-2kt} t^{n-2} (t+\tau)^{n-2} * dt \end{aligned}$$

Choose the time unit so that $T = 1$, one has

$$F_2 = e^{-\tau}$$

$$F_3 = e^{-2\tau} (1 + 2\tau)$$

$$F_4 = \frac{9}{8} e^{-3\tau} (1 + 3\tau(1 + \tau))$$

$$F_5 = \frac{1}{12} e^{-4\tau} (15 + 4\tau(15 + 8\tau(3 + 2\tau)))$$

$$F_6 = \frac{25}{384} e^{-5\tau} (21 + 5\tau(21 + 5\tau(9 + 5\tau(2 + \tau))))$$

AUTHOR CONTRIBUTIONS

JX conceived the project, constructed the model and wrote the paper with input from XT and HZ. XT performed most simulations. HZ collected biological background information and participated simulations. XT, HZ and JX analyzed the data.

ACKNOWLEDGMENTS

We thank Drs David Lyons and Andrew Chess for many helpful discussions. The research was supported by the U.S. National Science Foundation (DMS-0969417).

REFERENCES

- Alexander, J. M., and S. Lomvardas. 2014. "Nuclear architecture as an epigenetic regulator of neural development and function." *Neuroscience* 264:39-50. doi: 10.1016/j.neuroscience.2014.01.044.
- Alsing, A. K., and K. Sneppen. 2013. "Differentiation of developing olfactory neurons analysed in terms of coupled epigenetic landscapes." *Nucleic Acids Res* 41 (9):4755-64. doi: 10.1093/nar/gkt181.
- Bannister, A. J., and T. Kouzarides. 2011. "Regulation of chromatin by histone modifications." *Cell Res* 21 (3):381-95. doi: 10.1038/cr.2011.22.
- Buck, L., and R. Axel. 1991. "A Novel Multigene Family May Encode Odorant Receptors - a Molecular-Basis for Odor Recognition." *Cell* 65 (1):175-187. doi: Doi 10.1016/0092-8674(91)90418-X.
- Burgess, D. J. 2014. "Gene Regulation: Characterizing monoallelic expression." *Nat Rev Genet* 15 (3):143. doi: 10.1038/nrg3674.
- Chess, Andrew, Itamar Simon, Howard Cedar, and Richard Axel. 1994. "Allelic inactivation regulates olfactory receptor gene expression." *Cell* 78 (5):823-834. doi: [http://dx.doi.org/10.1016/S0092-8674\(94\)90562-2](http://dx.doi.org/10.1016/S0092-8674(94)90562-2).
- Dalton, R. P., D. B. Lyons, and S. Lomvardas. 2013. "Co-opting the unfolded protein response to elicit olfactory receptor feedback." *Cell* 155 (2):321-32. doi: 10.1016/j.cell.2013.09.033.
- Dodd, I. B., M. A. Micheelsen, K. Sneppen, and G. Thon. 2007. "Theoretical analysis of epigenetic cell memory by nucleosome modification." *Cell* 129 (4):813-22. doi: 10.1016/j.cell.2007.02.053.
- Ferreira, T., S. R. Wilson, Y. G. Choi, D. Risso, S. Dudoit, T. P. Speed, and J. Ngai. 2014. "Silencing of odorant receptor genes by G protein betagamma signaling ensures the expression of one odorant receptor per olfactory sensory neuron." *Neuron* 81 (4):847-59. doi: 10.1016/j.neuron.2014.01.001.
- Fuss, S. H., M. Omura, and P. Mombaerts. 2007. "Local and cis effects of the H element on expression of odorant receptor genes in mouse." *Cell* 130 (2):373-84. doi: 10.1016/j.cell.2007.06.023.
- Glusman, G., I. Yanai, I. Rubin, and D. Lancet. 2001. "The complete human olfactory subgenome." *Genome Res* 11 (5):685-702. doi: 10.1101/gr.171001.

- Godfrey, Paul A., Bettina Malnic, and Linda B. Buck. 2004. "The mouse olfactory receptor gene family." *Proceedings of the National Academy of Sciences of the United States of America* 101 (7):2156-2161. doi: 10.1073/pnas.0308051100.
- Goldbeter, A., and D. E. Koshland, Jr. 1981. "An amplified sensitivity arising from covalent modification in biological systems." *Proc Natl Acad Sci U S A* 78 (11):6840-4.
- Hathaway, N. A., O. Bell, C. Hodges, E. L. Miller, D. S. Neel, and G. R. Crabtree. 2012. "Dynamics and memory of heterochromatin in living cells." *Cell* 149 (7):1447-60. doi: 10.1016/j.cell.2012.03.052.
- Khan, M., E. Vaes, and P. Mombaerts. 2011. "Regulation of the probability of mouse odorant receptor gene choice." *Cell* 147 (4):907-21. doi: 10.1016/j.cell.2011.09.049.
- Kolterman, Brian E, Ivan Iossifov, and Alexei A Koulakov. 2012. "A race model for singular olfactory receptor expression." *arXiv preprint arXiv:1201.2933*.
- Lewcock, J. W., and R. R. Reed. 2004. "A feedback mechanism regulates monoallelic odorant receptor expression." *Proc Natl Acad Sci U S A* 101 (4):1069-74. doi: 10.1073/pnas.0307986100.
- Lomvardas, S., G. Barnea, D. J. Pisapia, M. Mendelsohn, J. Kirkland, and R. Axel. 2006. "Interchromosomal interactions and olfactory receptor choice." *Cell* 126 (2):403-13. doi: 10.1016/j.cell.2006.06.035.
- Lyons, D. B., W. E. Allen, T. Goh, L. Tsai, G. Barnea, and S. Lomvardas. 2013. "An epigenetic trap stabilizes singular olfactory receptor expression." *Cell* 154 (2):325-36. doi: 10.1016/j.cell.2013.06.039.
- Lyons, D. B., A. Magklara, T. Goh, S. C. Sampath, A. Schaefer, G. Schotta, and S. Lomvardas. 2014. "Heterochromatin-mediated gene silencing facilitates the diversification of olfactory neurons." *Cell Rep* 9 (3):884-92. doi: 10.1016/j.celrep.2014.10.001.
- Magklara, A., and S. Lomvardas. 2013. "Stochastic gene expression in mammals: lessons from olfaction." *Trends Cell Biol* 23 (9):449-56. doi: 10.1016/j.tcb.2013.04.005.
- Magklara, A., A. Yen, B. M. Colquitt, E. J. Clowney, W. Allen, E. Markenscoff-Papadimitriou, Z. A. Evans, P. Kheradpour, G. Mountoufari, C. Carey, G. Barnea, M. Kellis, and S. Lomvardas. 2011. "An epigenetic signature for monoallelic olfactory receptor expression." *Cell* 145 (4):555-70. doi: 10.1016/j.cell.2011.03.040.
- Markenscoff-Papadimitriou, Eirene, William E. Allen, Bradley M. Colquitt, Tracie Goh, Karl K. Murphy, Kevin Monahan, Colleen P. Mosley, Nadav Ahituv, and Stavros Lomvardas. 2014. "Enhancer Interaction Networks as a Means for Singular Olfactory Receptor Expression." *Cell* 159 (3):543-557.
- Nei, M., Y. Niimura, and M. Nozawa. 2008. "The evolution of animal chemosensory receptor gene repertoires: roles of chance and necessity." *Nat Rev Genet* 9 (12):951-63. doi: 10.1038/nrg2480.
- Nguyen, M. Q., Z. Zhou, C. A. Marks, N. J. Ryba, and L. Belluscio. 2007. "Prominent roles for odorant receptor coding sequences in allelic exclusion." *Cell* 131 (5):1009-17. doi: 10.1016/j.cell.2007.10.050.
- Peskin, C. S., G. M. Odell, and G. F. Oster. 1993. "Cellular motions and thermal fluctuations: the Brownian ratchet." *Biophys. J.* 65 (1):316-324.
- Plessy, C., G. Pascarella, N. Bertin, A. Akalin, C. Carrieri, A. Vassalli, D. Lazarevic, J. Severin, C. Vlachouli, R. Simone, G. J. Faulkner, J. Kawai, C. O. Daub, S. Zucchelli, Y. Hayashizaki, P. Mombaerts, B. Lenhard, S. Gustincich, and P. Carninci. 2012. "Promoter architecture of mouse olfactory receptor genes." *Genome Res* 22 (3):486-97. doi: 10.1101/gr.126201.111.
- Ressler, Kerry J., Susan L. Sullivan, and Linda B. Buck. 1993. "A zonal organization of odorant receptor gene expression in the olfactory epithelium." *Cell* 73 (3):597-609. doi: [http://dx.doi.org/10.1016/0092-8674\(93\)90145-G](http://dx.doi.org/10.1016/0092-8674(93)90145-G).

- Rodriguez-Gil, D. J., H. B. Treloar, X. Zhang, A. M. Miller, A. Two, C. Iwema, S. J. Firestein, and C. A. Greer. 2010. "Chromosomal location-dependent nonstochastic onset of odor receptor expression." *J Neurosci* 30 (30):10067-75. doi: 10.1523/JNEUROSCI.1776-10.2010.
- Serizawa, S., K. Miyamichi, H. Nakatani, M. Suzuki, M. Saito, Y. Yoshihara, and H. Sakano. 2003. "Negative feedback regulation ensures the one receptor-one olfactory neuron rule in mouse." *Science* 302 (5653):2088-94. doi: 10.1126/science.1089122.
- Shykind, B. M., S. C. Rohani, S. O'Donnell, A. Nemes, M. Mendelsohn, Y. Sun, R. Axel, and G. Barnea. 2004. "Gene switching and the stability of odorant receptor gene choice." *Cell* 117 (6):801-15. doi: 10.1016/j.cell.2004.05.015.
- Sim, C. K., S. Perry, S. K. Tharadra, J. S. Lipsick, and A. Ray. 2012. "Epigenetic regulation of olfactory receptor gene expression by the Myb-MuvB/dREAM complex." *Genes Dev* 26 (22):2483-98. doi: 10.1101/gad.201665.112.
- Tan, Longzhi, Chenghang Zong, and X. Sunney Xie. 2013. "Rare event of histone demethylation can initiate singular gene expression of olfactory receptors." *Proceedings of the National Academy of Sciences*. doi: 10.1073/pnas.1321511111.
- Vassar, R., J. Ngai, and R. Axel. 1993. "Spatial segregation of odorant receptor expression in the mammalian olfactory epithelium." *Cell* 74 (2):309-18.
- Vosshall, L. B., H. Amrein, P. S. Morozov, A. Rzhetsky, and R. Axel. 1999. "A spatial map of olfactory receptor expression in the *Drosophila* antenna." *Cell* 96 (5):725-36. doi: 10.1016/s0092-8674(00)80582-6.
- Weth, F., W. Nadler, and S. Korsching. 1996. "Nested expression domains for odorant receptors in zebrafish olfactory epithelium." *Proc Natl Acad Sci U S A* 93 (23):13321-6.
- Zhang, H., X. J. Tian, A. Mukhopadhyay, K. S. Kim, and J. Xing. 2014. "Statistical mechanics model for the dynamics of collective epigenetic histone modification." *Phys Rev Lett* 112 (6):068101.
- Zhang, X., and S. Firestein. 2002. "The olfactory receptor gene superfamily of the mouse." *Nat Neurosci* 5 (2):124-33. doi: 10.1038/nn800.

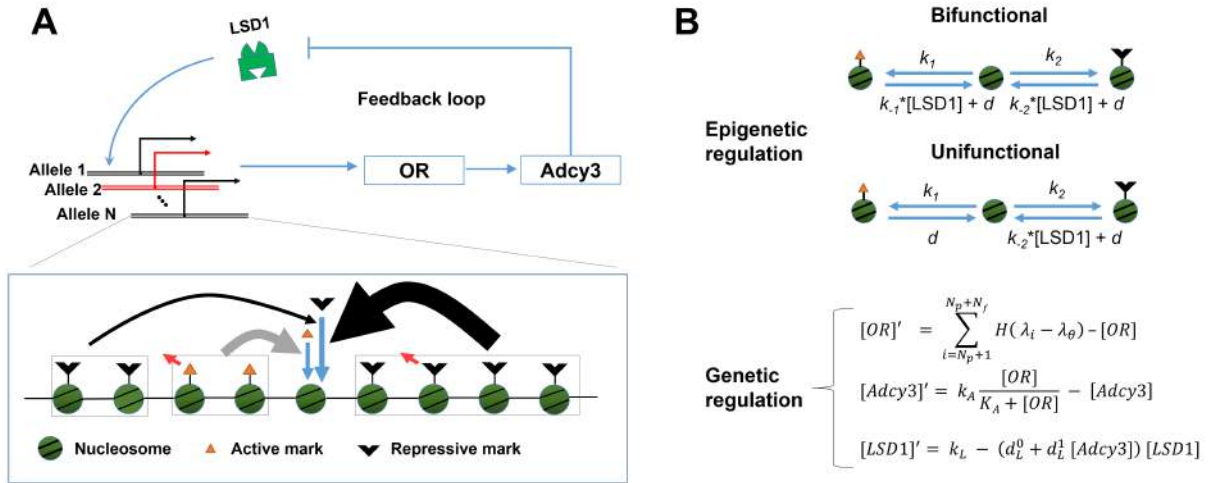


Figure 1. Mathematical model of the experimentally revealed regulatory system of olfactory receptor activation. (A) Feedback regulated OR allele epigenetic activation. Each OSN contains N_p ($= 30$) pseudo OR alleles and N_f ($= 70$) functional OR alleles. Each allele is composed of a linear array of 41 nucleosomes. Each nucleosome bears active, no, or repressive mark, and a mark-bearing nucleosome facilitates an empty nucleosome to add the same mark in a distance dependent manner. Expression of an OR protein elicits a feedback to induce expression of enzyme Adcy3, which removes the demethylase LSD1. (B) The corresponding mathematical formulation. A nucleosome changes its covalent modification state stochastically with the indicated rate constants. The methylation rate constants k_1 and k_2 are influenced by nearby nucleosomes. Protein level changes are simulated by ordinary differential equations. $H(x)$ is a Heaviside function which assumes value 0 for $x < 0$, and 1 otherwise. λ_i is the fraction of active mark in allele i , while λ_θ is the cutoff fraction of nucleosomes with active marks so an allele is regarded as epigenetically activated.

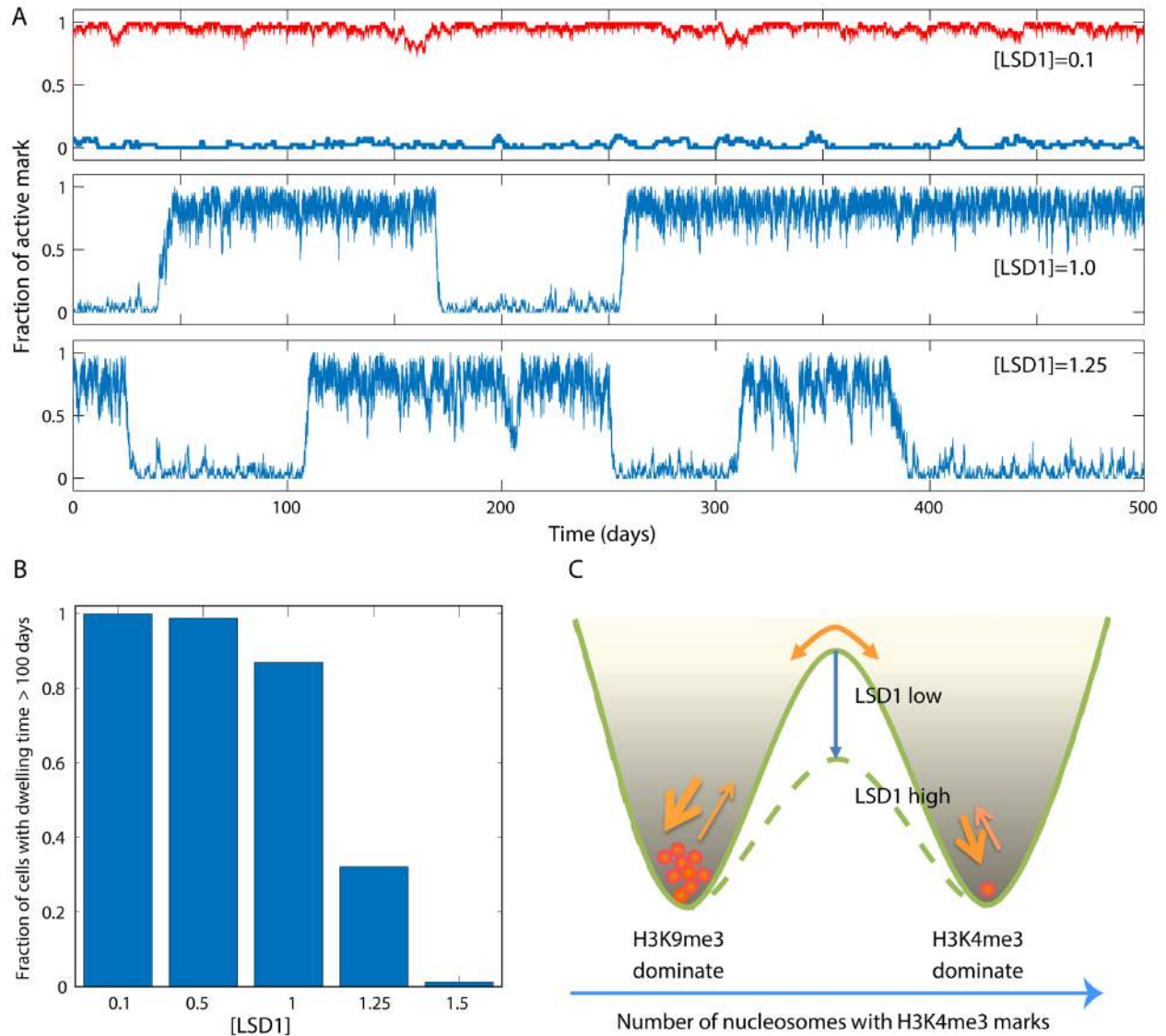


Figure 2. Low Noise and demethylation enzyme concentration kinetically freeze allele epigenetic state. (A) Typical single allele trajectories of the fraction of nucleosomes with active marks under various constant concentrations of LSD1. (B) The fraction of alleles that maintain epigenetic state longer than 100 days under various constant concentrations of LSD1. The result was sampled over 1000 alleles initially in the collective repressive mark dominated state. (C) Analogous double-well potential system with the barrier height inversely related to LSD1 concentration.

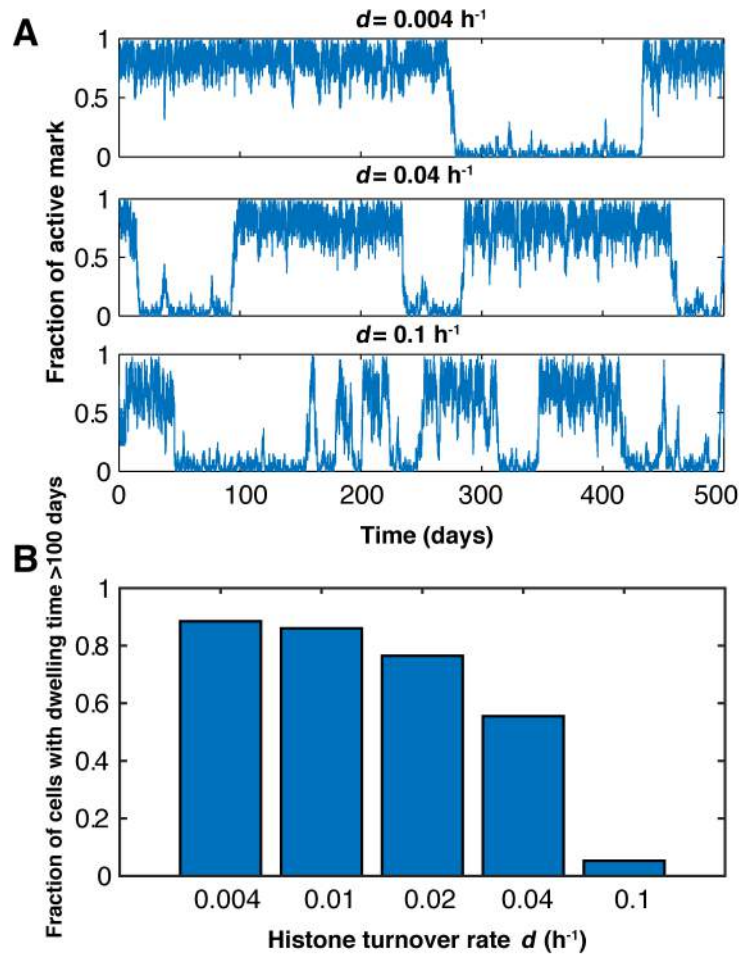


Figure 2 supplement 1. Low histone turnover rate stabilizes the epigenetic state of an allele.

(A) Typical trajectories of the epigenetic state of an allele with different values of the histone turnover rate. (B) The fraction of alleles that maintain epigenetic state within 100 days as a function of the histone turnover rate d .

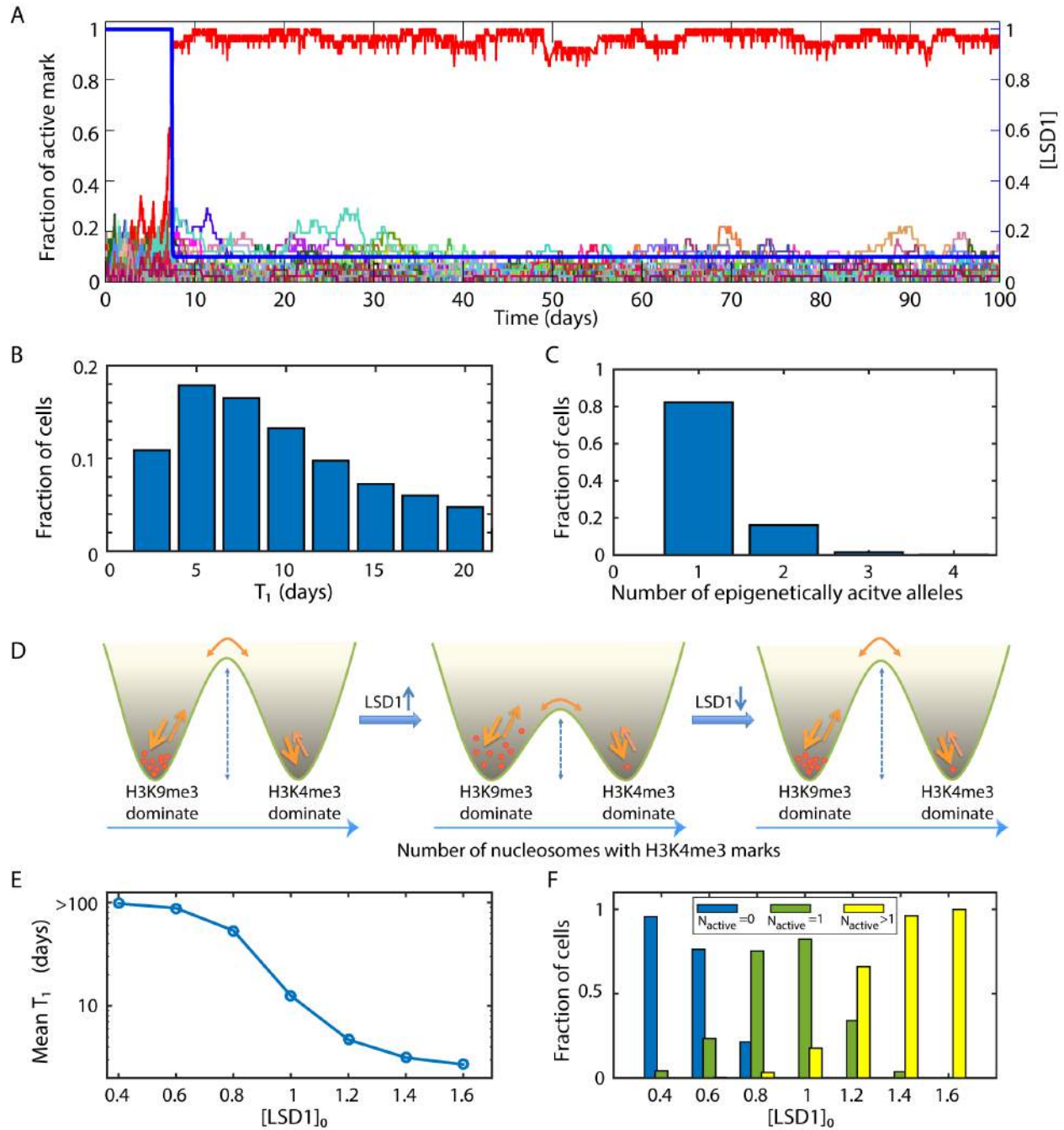


Figure 3. Bifunctional LSD1 leads to barrier-crossing-like dynamics and ensures mono-allelic epigenetic activation. (A) Typical trajectories of the fraction of nucleosomes with active marks on one allele for 100 alleles (represented by different colors) within a cell. The temporal change of LSD1 level (blue curve, in relative unit) is also indicated. (B) Distribution of

T_1 , the time observing the first epigenetically active allele (75% nucleosomes bearing active marks). Sampled over 1000 cells. (C) Fraction of cells with various numbers of epigenetically active alleles at day 100. (D) The analogous potential system during activation. (E) Dependence of the average of T_1 on the elevated LSD1 level ($[LSD1]_0$) during differentiation. (F) Dependence of the fraction of cells with various numbers of epigenetically active alleles at day 100 on $[LSD1]_0$. In all simulations a cell has 100 OR alleles, and at time 0 the LSD1 level is elevated 10 folds from its basal value to simulate the onset of differentiation.

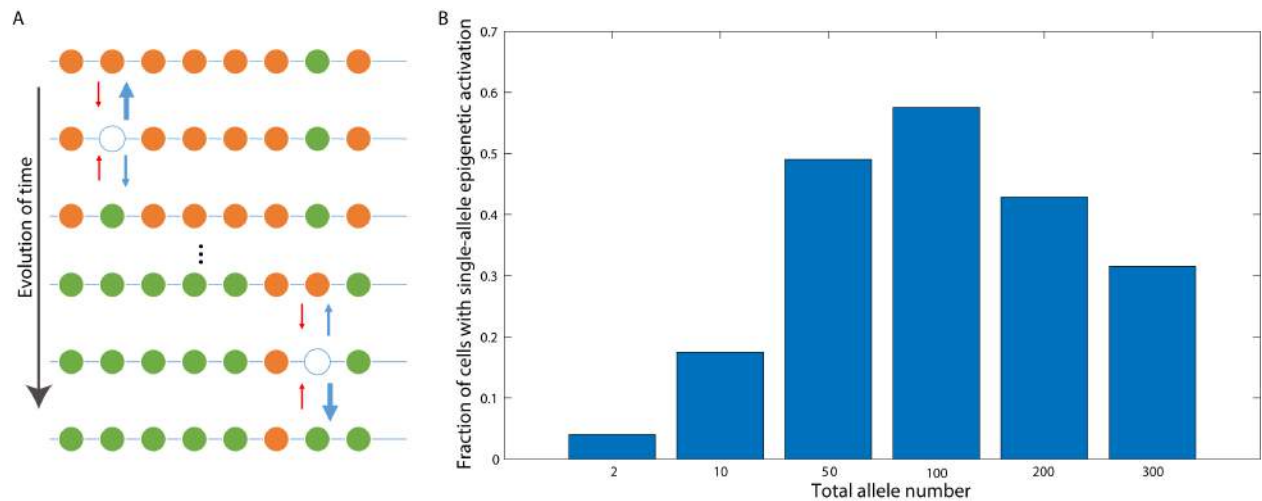


Figure 3 supplement 1. Additional results of bifunctional LSD1 elicited epigenetic conversion. (A) Schematic illustration of a conversion process elicited by bifunctional LSD1. Orange, green, and white balls represent nucleosomes bearing repressive, active, and no marks, respectively. The widths of arrows represent the relative values of corresponding rates. (B) The monoallelic ratio changes non-monotonically over the number of the allele. Except for the total number of alleles, the simulations are performed in the same way as those in Figure 3D.

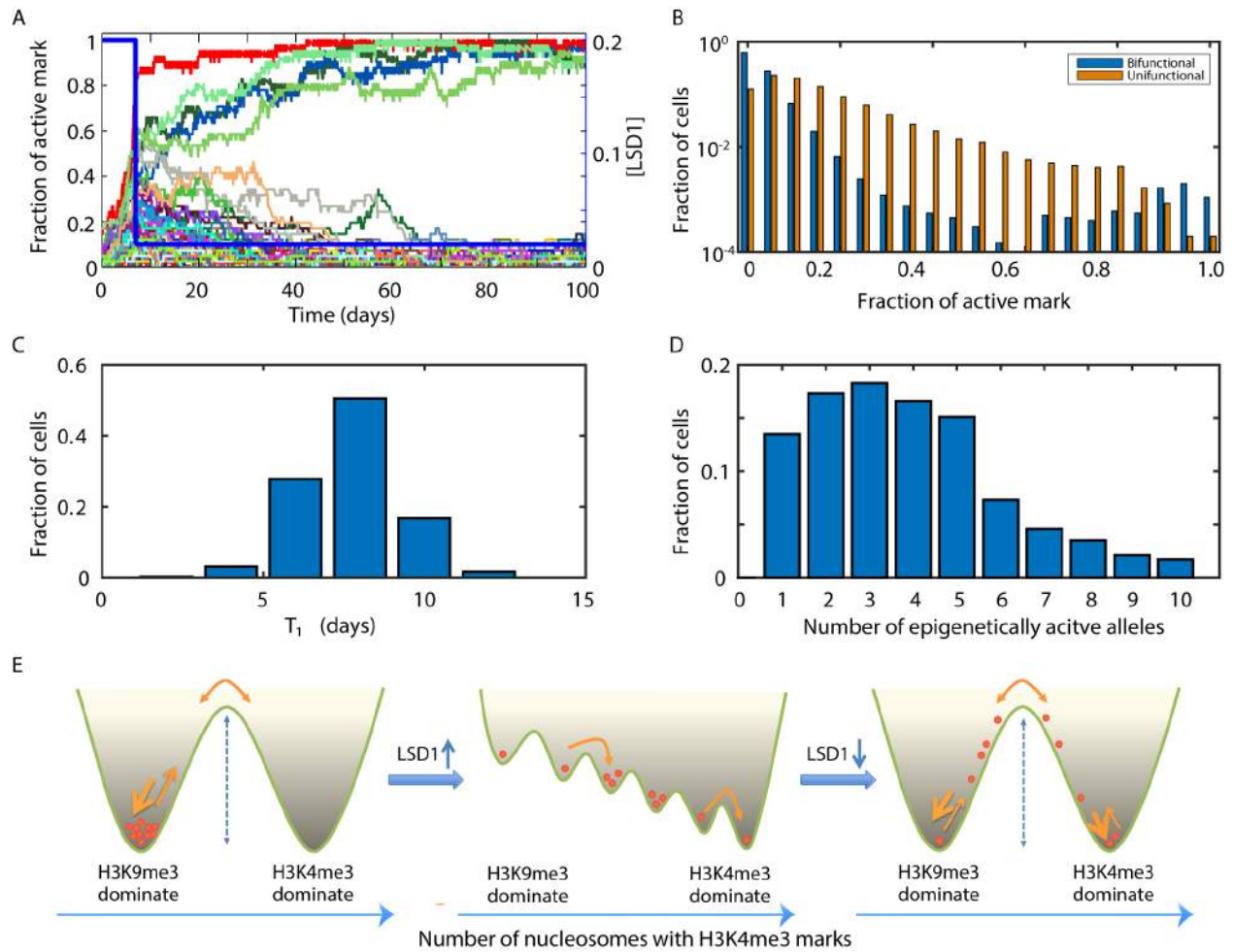


Figure 4. Unifunctional LSD1 leads to ratchet-like dynamics and cannot ensure mono-allelic epigenetic activation. (A) Typical trajectories of the fraction of nucleosomes with active marks on one allele for 100 alleles within a cell. The temporal change of LSD1 level is also indicated. (B) Distribution of the fraction of nucleosomes with active marks on day 8 with bifunctional and unifunctional LSD1. Sampled over 1000 cells. (C) Distribution of T_1 . Sampled over 1000 cells. (D) Fraction of cells with various numbers of epigenetically active alleles at day 100. (E) The analogous potential system during activation.

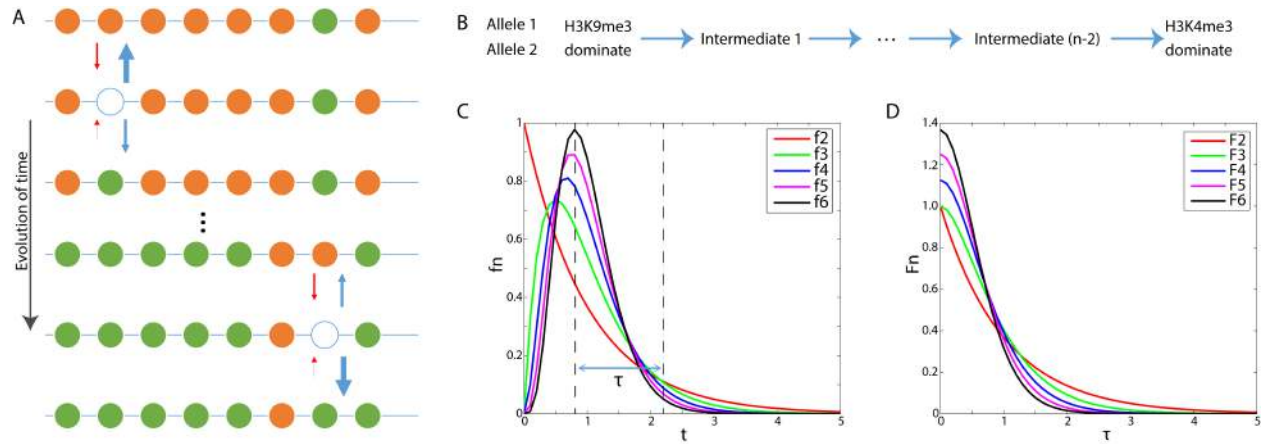


Figure 4 supplement 1. Simple mathematical analysis reveals the mechanistic advantage of bidirectional over unidirectional demethylation enzyme. (A) Schematics of a conversion process elicited by unifunctional LSD1. Same notations as in Figure 3 supplement 1A. (B) Minimal effective Markovian transition models for an OR allele changing from H3K9me3 dominate state to H3K4me3 dominate state with no ($n = 2$, corresponding to the barrier-crossing dynamics with the bifunctional LSD1), and various number ($n > 2$, corresponding to the ratchet-like dynamics with the unifunctional LSD1) of intermediate states. Here we compare two independent alleles that undergo the transition. (C) The first-arrival time (t) distribution f_n of a single allele transiting from H3K9me3 dominate state to H3K4me3 dominate state as a function of the overall state number n . (D) The distribution (F_n) of first-arrival time separation (τ) between two kinetically independent alleles as a function of the overall state number n . From engineering design perspective a larger τ is desirable since it gives the system more response time to elicit the feedback after the first allele becomes epigenetically active and prevents the second allele from making the transition.

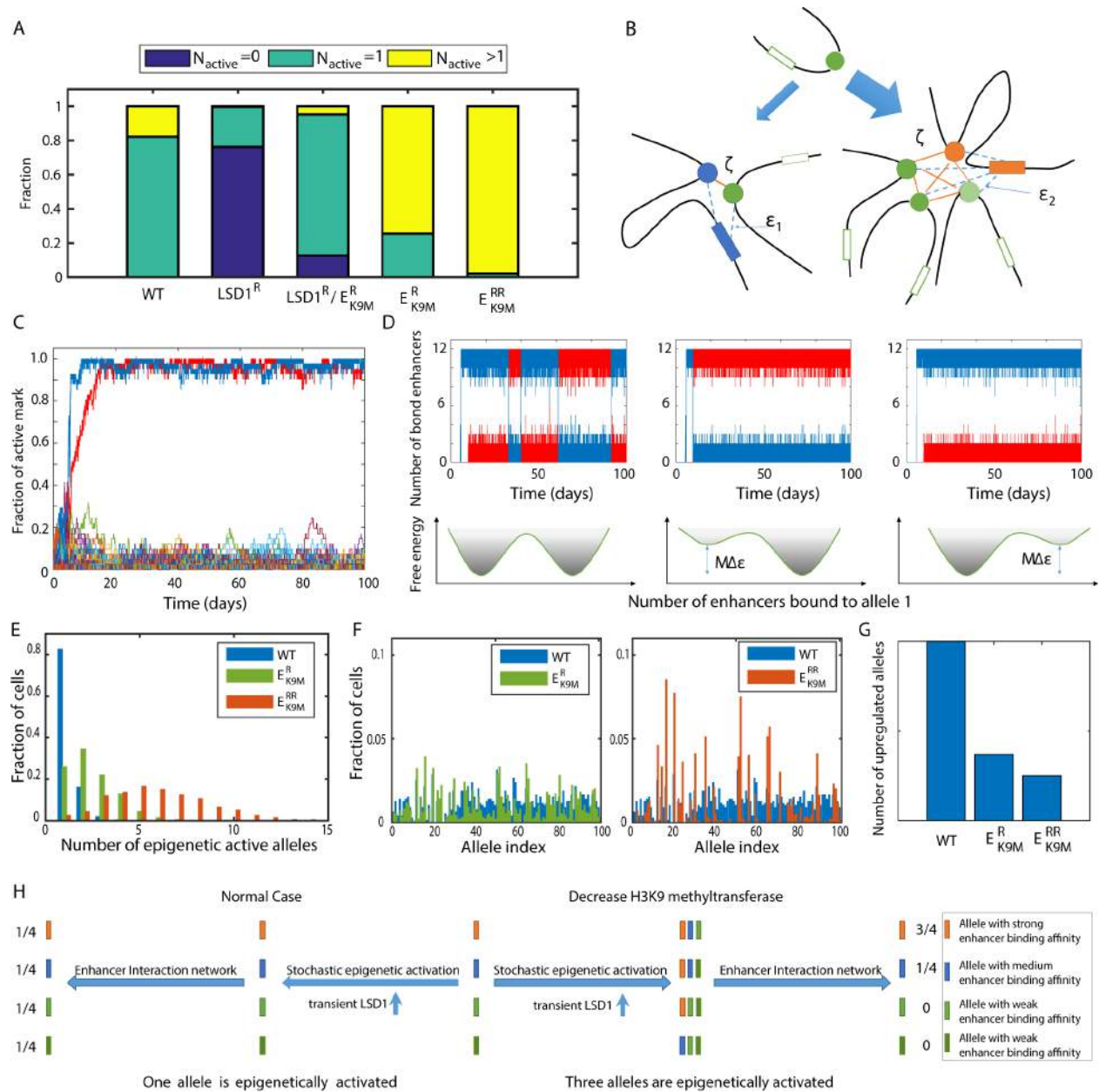


Figure 5. Competition of cooperatively bound enhancers further reduces co-expression of multi-allele ORs. (A) Predicted fractions of cells with various numbers of epigenetic active alleles under different conditions. WT: wide type. $LSD1^R$: LSD1 level reduced. E_{K9M}^R/E_{K9M}^{RR} : H3K9 methyltransferase level reduced and further reduced. (B) Model of alleles competing for M enhancers. (C) Simulated allele trajectories of one cell with two epigenetically active alleles. (D) Simulated dynamics of enhancers binding to two epigenetic active alleles corresponding to

the cell in panel C with the same (left) or different (by $\Delta\varepsilon = \pm 0.5 k_B T$, middle and right) binding affinity. Also shown are schematic free energy profiles. (E) Simulated distribution of 1000 cells with various numbers of epigenetically active alleles under E_{K9M}^R , E_{K9M}^{RR} and WT on day 100. (F) Fractions of overall protein expression of each allele simulated with a population of 1000 cells under E_{K9M}^R and E_{K9M}^{RR} comparing to those with WT. (G) The number of transcriptionally upregulated alleles under E_{K9M}^R , E_{K9M}^{RR} and in WT. (H) Schematic illustration on the mechanism of reduced OR expression diversity with E_{K9M}^R and E_{K9M}^{RR} compared to that in WT.

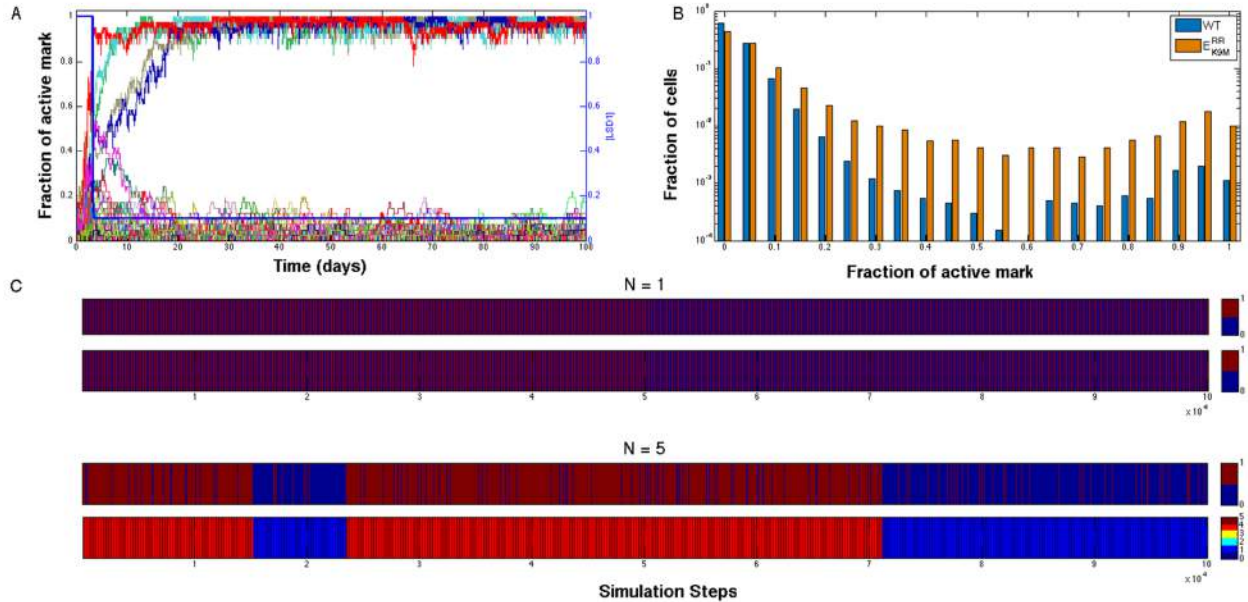


Figure 5 supplement 1. Enhancer competition assures transcriptional activation of single allele. (A) Typical single-allele trajectories of the fraction of nucleosomes with active marks for 100 allele within an E_{K9M}^R cell. (B) The distribution of the fraction of nucleosomes with active marks on day 8 averaged over 1000 cells. (C) Auxiliary enhancers stabilize binding of a specific enhancer to an allele. For each result with M enhancers, the upper one shows the trajectory of enhancer 1, and the lower one shows the corresponding number of enhancers bound to allele 1. The time is given by the number of Gillespie simulation steps. In these simulations, $\varepsilon_1 = \varepsilon_2 = -1 k_B T$, $\zeta = -3 k_B T$. Similar results were obtained with broad range of parameter values (*e.g.*, $\varepsilon_1/\varepsilon_2$ assuming values -2 to $-0.5 k_B T$ and ζ -3 to $-0.5 k_B T$), and more enhancers involved.

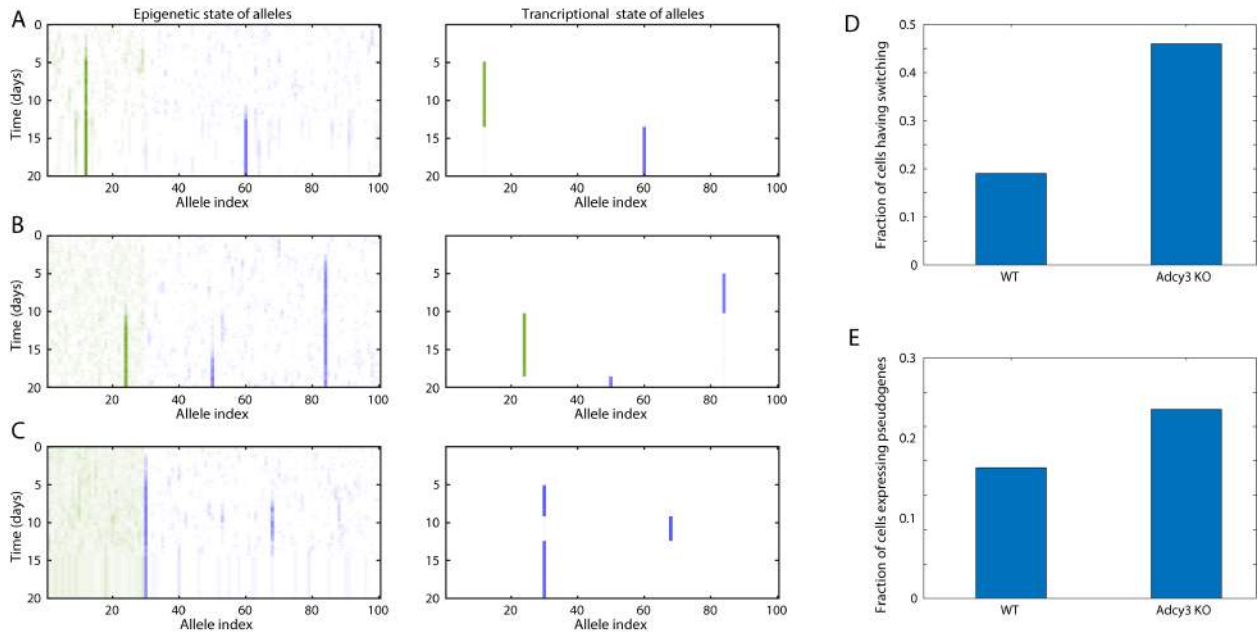


Figure 6. Predicted OR expression switching schemes. Typical switching examples: active pseudo gene switches to intact gene (A), active intact gene switches to pseudo gene and then switches to intact gene (B), and intact active gene switch off itself (C). (D) Simulated switching frequency under WT and Adcy3 KO conditions. (E) Simulated fraction of cells expressing pseudo genes under WT and Adcy3 KO conditions.

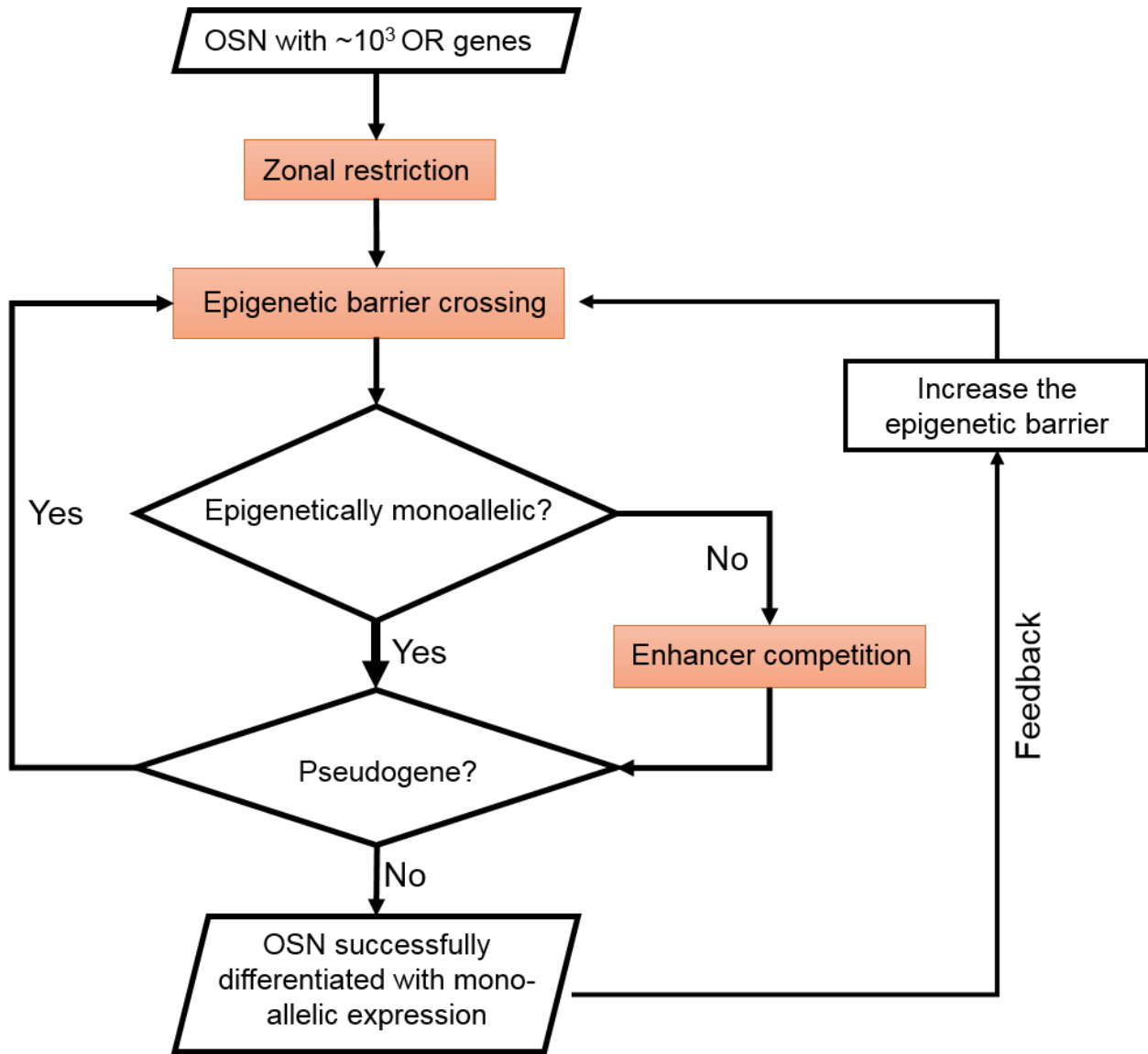


Figure 7. The three-layer mechanism ensures mono-allele activation of OR genes.

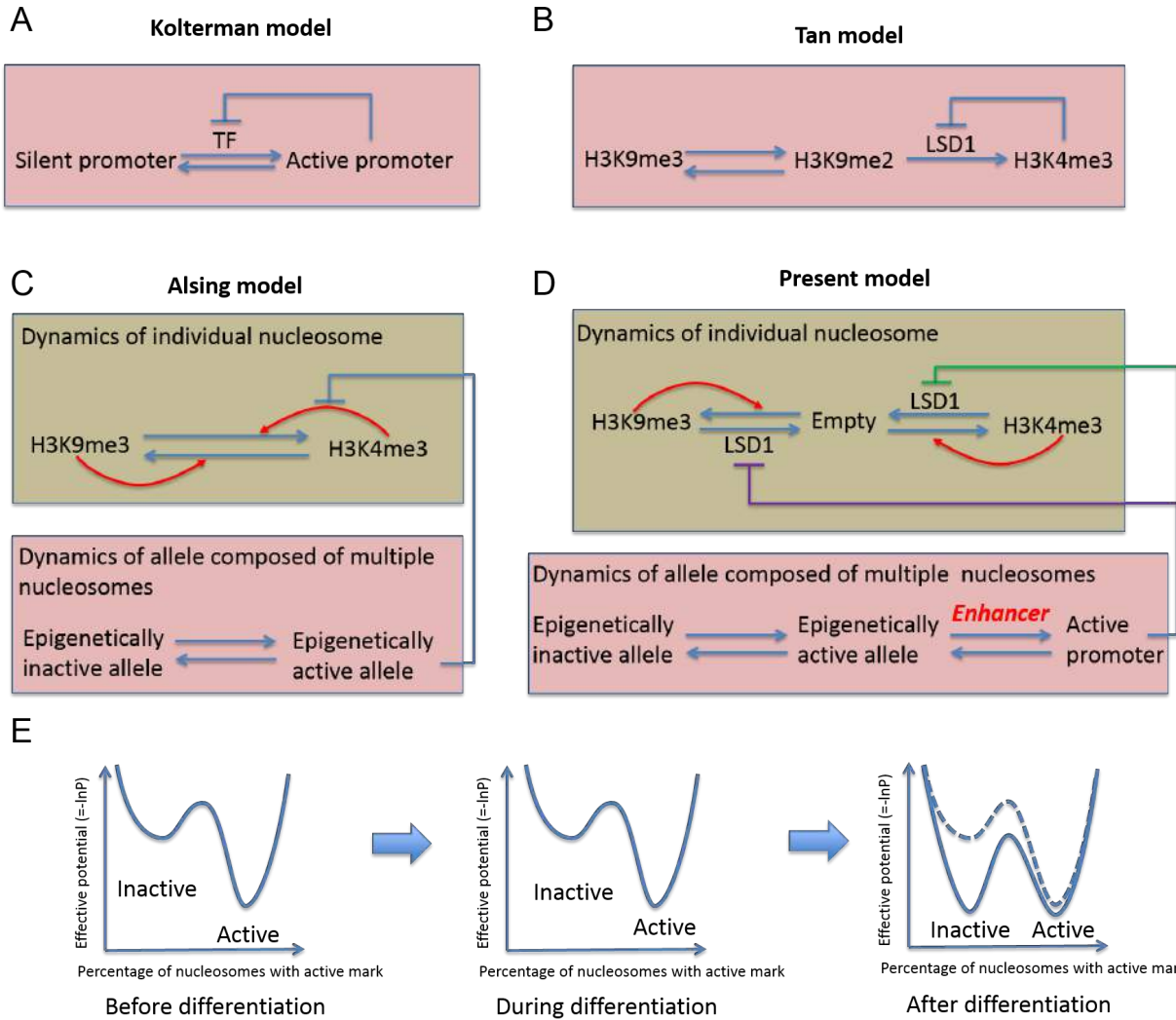


Figure 7 supplement 1. Comparison of existing mathematical models. (A) In the model of Kolterman et al. (Kolterman, Iossifov, and Koulikov 2012), OR promoters compete for cooperative binding of a limited number of transcription factors, and OR expression elicits a feedback to degrade the transcription factors. While the mechanism is not consistent with known experimental information, the model suggests the importance of cooperative binding of trans-elements. (B) The model of Tan et al. (Tan, Zong, and Xie 2013) assumes that the transcriptional activity of an OR allele is controlled by the epigenetic state of one nucleosome in the promoter region. A slow LSD1-dependent $\text{H3K9me2} \rightarrow \text{H3K4me3}$ transition is controlled by a fast feedback that removes LSD1. Notice that the transition is irreversible and LSD1 is considered

unifunctional. (C) Alsing et al. (Alsing and Sneppen 2013) considers that each allele is composed of a number of nucleosomes. Each nucleosome exists as H3K9me3 or H3K4me3, and the transition is affected by other nucleosomes as positive feedbacks. A negative feedback elicited by the expressed OR decreases the H3K9me3→H3K4me3 transition rate. (D) The present model also considers that each allele is composed of a number of nucleosomes. Treating each nucleosome dynamics as transitions among three states, the model is able to examine the role of bifunctional LSD1. The feedback affects both H3K9 and H3K4 demethylation. Furthermore an epigenetically active allele needs to bind enhancers to become transcriptionally active. A hypothetical unifunctional LSD1 model differs only in absence of the negative feedback on H3K4 demethylation (the green line and dependence of demethylation on LSD1), but generates qualitatively different dynamics. (E) Analogous potential system corresponding to the Alsing model. Initially the inactive well is shallower than the active well, reflecting the requirement that for mice OSN differentiation takes place in 5-10 days, but the choice needs to be maintained for ~3 months. The feedback reduces the rate of H3K9me3→H3K3me3 transition, and thus stabilizes the inactive well while slightly destabilizes the active well.

Table S1 Model predictions and corresponding experimental confirmations and suggestions. Confirmed predictions are shown as shaded.

Model predictions	Experimental confirmation or suggestions
OSNs need to maintain saturating levels of methyltransferases, but low levels of demethylases and stochastic histone exchange rate before and after differentiation (Fig.2 and Fig. 2 Supplement 1) .	Compare the enzyme levels and histone exchange rate (e.g., using isotope labeled histones) within OSNs and other types of cells.
The number of OR alleles in a zone affects the single-allele ratio nonmonotonically (Fig. 3B).	
Decreasing LSD1 concentration impedes OR activation (less OSN differentiation), which can be partially restored by inhibiting G9a/GLP.	Confirmed in mice (Lyons et al. 2014).
Epigenetic switching assumes a barrier-crossing-like dynamics for WT (Fig. 3, Fig. 4B), but a ratchet-like dynamics with G9a/GLP dKO (Fig. 5 Supplement1 A &B).	Following Magklara et al. (Magklara et al. 2011), sort GFTP+ cells from OMP-IRES-GFP mice, and perform CHIP-qPCR for selected silent OR genes. Perform similar studies with OMP-IRES-GFP and G9a/GLP dKO mice. We predict that silent OR alleles from the former are dominated by H3K9me3, but those from the latter have mixed nucleosomes with H3K4 and H3K9 methylations. One can further measure the epigenetic pattern at different time points before and after differentiation to test the prediction that it takes long time for the alleles with mixed methylations to relax to one of the epigenetic states with one mark dominated.
A cell may have more than one epigenetically active alleles (Fig. 3F).	Following Shykind et al.(Shykind et al. 2004), cross mice bearing MOR28-IRES-Cre allele with strains bearing the reporter Rosa-loxP-stop-loxP-CFP, sort CFP+Cre- cells and perform epigenetic histone modification analysis as in Magklara et al.(Magklara et al. 2011).
Inhibition of H3K9 methyltransferases G9a/GLP leads to multiple allele activation (Fig. 5A).	Confirmed in Zebrafish (Ferreira et al. 2014) and mice (Lyons et al. 2014).
With enhancer competition, Inhibition of H3K9 methyltransferases G9a/GLP leads to transcriptional downregulation of most OR genes upregulation of a small number of genes, and thus lead to decrease of diversity of expressed OR genes (Fig. 5E-G).	Confirmed in mice (Lyons et al. 2014).
Multiple epigenetically active alleles compete for a finite number of enhancers, which contributes to the diversity reduction in G9a/GLP KO mice (Fig. 5).	Introduce enhancers ectopically to G9a KO mice (Lomvardas et al., 2006), which should at least partially rescue the reduction of OR diversity if the model holds.
The proximity difference of enhancers to a gene	Replace an upregulated OR gene together with the

leads to different OR-enhancer binding strength.	promoter by a down-regulated one, and test whether the latter becomes upregulated in a G9a/GLP dKO MOE.
The binding strength differences between an OR promoter and individual enhancers can be small thus experimentally hard to detect, but are amplified by cooperative enhancer binding (Fig. 5D).	Lyon <i>et al.</i> could not identify any significant differences between the promoters of the most upregulated ORs and the remaining ones in predicting the transcription-factor-binding-motifs (Lyons et al. 2014)
The switching frequency increases in Adcy3 KO OSNs compared to that in WT OSNs (Fig. 6D). Furthermore, the fraction of cells expressing pseudo ORs increases while that expressing functional ORs decreases in Adcy3 KO mice (Fig. 6E).	Confirmed (Lyons et al. 2013)
The genes showing upregulated expression in the G9a/GLP dKO mice, such as Olfr231, have slighter stronger interactions with the enhancers than the remaining genes do. Then in normal mice, OSNs that express one of these genes should have lower frequency of switching than those cells express other genes in the same zone do.	Follow the study procedure of Shykind et al.(Shykind et al. 2004). It can reveal more information if one use techniques such as the CRISPR-Cas9 gene editing approach to fluorescently label genes like Olfr231, and perform time-lapse studies.

Table S2 Values of model parameters used in this work.

Parameter	Value
Active mark methylation rate constant k_1	within nucleation region 0.125 h^{-1} , outside nucleation region 0.025 h^{-1} .
Repressive mark methylation rate constant k_2	within nucleation region, 0.125 h^{-1} (WT), outside nucleation region, 0.025 h^{-1} (WT)
Active mark demethylation rate constant k_{-1}	0.125 h^{-1}
Repressive mark demethylation rate constant k_{-2}	0.125 h^{-1}
Nucleosome correlation length μ	0.64
Histone turnover rate d	0.002 h^{-1}
Cutoff fraction of nucleosomes with active marks so an allele is regarded as epigenetically activated λ_θ	0.75
Adcy3 synthesis rate k_A	1 h^{-1}
Michaelis-Menten constant of OR induced Adcy3 expression K_A	0.8
LSD1 basal degradation rate constant d_L^0	0.5 h^{-1}
Adcy3 facilitated LSD1 degradation rate constant d_L^1	8 h^{-1}
Prefactor for the enhancer switching rate constant ν^*	1 h^{-1}
Free energy of enhancer-enhancer interaction ς	$-0.5 k_B T$
Free energy of enhancer-allele interaction ε	$\sim -1 k_B T$
Total number of enhancers M	12

* This parameter is only used in generating Figure 5D for illustration purpose, and its actual value can be better estimated if time-course of OR switching becomes available.